Li and Lv
Future Journal of Pharmaceutical Sciences (2024) 10:30
https://doi.org/10.1186/s43094-024-00605-5

Future Journal of
Pharmaceutical Sciences

RESEARCH

Open Access

Cordycepin alleviates osteoarthritis by inhibiting chondrocyte ferroptosis via Keap1/Nrf2 axis

Jianlei Li[1*] and Zuo Lv[1]

Abstract

Background Intervertebral disc degeneration (IVDD) is a prevalent condition known to contribute to lower back pain and various spinal disorders. The progression of IVDD is closely associated with cell ferroptosis. This study aimed to explore the therapeutic potential of a reactive oxygen species (ROS)-responsive hydrogel loaded with garlic extract for the inhibition of cell ferroptosis and the treatment of IVDD.

Results The study encapsulated garlic extract within the hydrogel using physical entrapment and controlled the release of the extract through the ROS-responsive degradation of the hydrogel. Our findings revealed that the hydrogel effectively inhibited the ferroptosis of nucleus pulposus cells induced by hydrogen peroxide. Furthermore, the hydrogel, when loaded with garlic extract, notably downregulated the expression of pro- ferroptosis genes and upregulated the expression of anti- ferroptosis genes.

Conclusions This study demonstrated that the hydrogel loaded with garlic extract significantly mitigated IVDD. These results highlight the promising potential of ROS-responsive hydrogel loaded with garlic extract as a viable treatment option for addressing IVDD.

Keywords Cordycepin, Ferroptosis, Osteoarthritis

Background

Osteoarthritis (OA) is a prevalent chronic joint disorder characterized by the progressive degeneration of articular cartilage, remodeling of subchondral bone, and inflammation of the synovium [1]. With a prevalence of approximately 10% worldwide, it ranks among the most common musculoskeletal conditions [2]. OA is a complex ailment influenced by a combination of genetic, mechanical, and biochemical factors. Advanced age, obesity, and joint injuries are recognized as risk factors that contribute to the onset and progression of OA [3, 4]. Given the projected substantial increase in the global burden of OA in the near future, it has become a significant public health concern.

Ferroptosis is a regulated form of cell death characterized by the accumulation of lipid peroxides and reactive oxygen species (ROS), which ultimately leads to cell membrane damage and subsequent cell death. This distinct process stands apart from other known forms of cell death, including apoptosis and necrosis. It has gained recognition as a significant contributor to various human diseases, such as neurodegeneration, cancer, and cardiovascular diseases [5–7].

The Kelch-like ECH-associated protein 1 (Keap1)/nuclear factor erythroid 2-related factor 2 (Nrf2) pathway plays a crucial role in regulating oxidative stress and maintaining cellular redox homeostasis [8]. Keap1, located in the cytoplasm, normally interacts with the transcription factor Nrf2 and promotes its degradation through the ubiquitin–proteasome system under

*Correspondence:
Jianlei Li
lijianlei_sx@163.com
[1] Department of Orthopedics Surgery, Shaoxing People's Hospital, Shaoxing, Zhejiang, China

normal conditions [9]. Upon exposure to oxidative stress or electrophilic agents, Keap1 undergoes conformational changes, leading to the stabilization and activation of Nrf2. Subsequently, Nrf2 translocates to the nucleus where it binds to the antioxidant response element (ARE), resulting in the transcriptional upregulation of various cytoprotective genes, including heme oxygenase-1 (HO-1), glutathione peroxidase (GPx), and solute carrier family 7 member 11 (SLC7A11) [10, 11].

Recent studies have demonstrated a close association between the Keap1/Nrf2 pathway and ferroptosis, highlighting its dysregulation as a potential contributor to the pathogenesis of diverse diseases [12]. For instance, in cancer, the constitutive activation of the Keap1/Nrf2 pathway has been demonstrated to enhance tumor growth and confer resistance to chemotherapy through the inhibition of ferroptosis [13]. Conversely, the activation of the Keap1/Nrf2 pathway has been demonstrated to confer protection against ferroptosis-induced cell death across diverse cell types, including neurons, cardiomyocytes, and chondrocytes [14–16]. The involvement of ferroptosis and the Keap1/Nrf2 pathway in osteoarthritis remains poorly understood, necessitating further research to elucidate their respective contributions to the progression of the disease. Nonetheless, emerging studies propose the involvement of ferroptosis in articular cartilage degeneration and indicate the therapeutic potential of activating the Keap1/Nrf2 pathway in averting cartilage destruction in osteoarthritis.

Cordycepin, known scientifically as 3'-deoxyadenosine, is a notable compound isolated from the caterpillar fungus Cordyceps militaris [17]. Historically utilized in traditional Chinese medicine, cordycepin has witnessed a resurgence in scientific interest due to its diverse pharmacological properties, including anti-inflammatory, antioxidant, and anticancer effects [17–19]. This resurgence is supported by a systematic approach to reviewing its biological activities, reflecting a growing recognition of its potential as a therapeutic agent. Notably, cordycepin's structural similarity to adenosine—a key signaling molecule—underpins its broad physiological functions, ranging from immune system activation to potential anticancer activities [20]. Its mechanism of action includes modulation of cell survival, proliferation, migration, and inflammation, positioning cordycepin as a promising candidate for addressing complex diseases like osteoarthritis [21]. Research indicates that cordycepin may treat OA by regulating autophagy and oxidative stress levels, thereby inhibiting the expression of cartilage inflammation [22–24]. Nevertheless, the potential therapeutic effects of cordycepin on OA and its underlying mechanism of action remain incompletely understood. Ziwen Wang et al., suggest cordycepin modulates the Keap1/Nrf2 pathway, inhibiting cellular senescence in rodents [25]. This leads to the hypothesis that cordycepin could regulate the Keap1/Nrf2 pathway to inhibit chondrocyte ferroptosis, potentially improving OA conditions.

In this study, we aimed to investigate the impact of cordycepin on OA pathogenesis and chondrocyte ferroptosis. Our findings demonstrate that cordycepin can alleviate symptoms of OA by inhibiting ferroptosis in chondrocytes through the modulation of the Keap1/Nrf2 pathway. These findings offer novel insights into the molecular mechanisms driving OA pathogenesis and propose cordycepin as a promising therapeutic agent for this condition.

Methods

In vitro experiments

Isolation and culture of chondrocytes

One-week-old C57BL/6 mice were euthanized and disinfected by immersion in 75% alcohol. Using aseptic techniques, an incision was made in the skin and soft tissue surrounding the knee joint of the hind leg to expose the knee joint. The femoral condylar cartilage was excised, minced, and immersed in a Phosphate-Buffered Saline (PBS) solution supplemented with 1% penicillin and streptomycin for 15 min. Subsequently, the tissue was transferred to Dulbecco's modified eagle's Medium (DMEM) culture medium supplemented with 0.2% collagenase and 5% Fetal Bovine Serum (FBS) and subjected to digestion for 6 h at 37 °C. Collagenase is employed to digest the extracellular matrix for the efficient extraction of chondrocytes and FBS is incorporated into the culture medium to provide vital nutrients, growth factors, and hormones necessary for the optimal growth and maintenance of the cultured chondrocytes. After digestion, the resulting solution was centrifuged at 1200 rpm for 10 min, and the resulting precipitate was collected. The cells were then suspended in DMEM culture medium supplemented with 5% FBS and cultured at 37 °C under 5% carbon dioxide conditions for subsequent passages.

Cytotoxicity evaluation of cordycepin using the cell counting kit-8 (CCK-8) assay

In the cytotoxicity evaluation of cordycepin using the CCK-8 assay, chondrocytes were seeded at an initial density of 5,000 cells per well in 12-well plates. This seeding density was chosen to achieve logarithmic growth phase within 72 h of culture. The chondrocytes at passage number 3 were treated with DMEM/FBS medium supplemented with cordycepin at concentrations of 0, 10, 20, 40, 80, and 160 μg/mL for a duration of 72 h. In the treatment phase, the DMEM/FBS medium used for chondrocyte culture was composed of DMEM supplemented with 10% FBS, 1% penicillin–streptomycin. Subsequently,

for the cytotoxicity evaluation, the CCK-8 solution (MCE, No. HY-K0301)was used at a final concentration of 10 μL per well and the cells were incubated for 2 h. The CCK-8 assay employs a water-soluble tetrazolium salt to produce a colorimetric change in response to cellular metabolic activity, allowing for the quantification of cell viability. The absorbance at 490 nm of each well was measured using an enzyme-linked instrument. The relative cell viability of each group was determined relative to the control group treated with 0 μg/mL cordycepin.

Measurement of Fe2 + content in chondrocytes

The Fe2 + content in chondrocytes was quantified using an Fe2 + assay kit (Elabscience, No. E-BC-F101). This assay kit is specifically designed to quantitatively determine Fe2 + levels in biological samples through a colorimetric assay, leveraging a specific ligand that forms a colored complex with Fe2 +. Chondrocytes from each group were collected, washed three times with PBS, and subsequently homogenized in an iron detection buffer. Subsequently, 5 μL of iron reductant and 5 μL of assay buffer were added to the standard well, and the resulting mixture was incubated for 30 min. The iron detection buffer provided with the Fe2 + Assay Kit, is formulated to optimize the conditions for Fe2 + ion interaction with the colorimetric probe, enhancing the specificity and sensitivity of the assay. Its composition ensures the stabilization of Fe2 + ions and prevents oxidation, thereby contributing to the precise quantification of Fe2 + levels. Following that, 100 μL of iron probe was added, mixed thoroughly, and incubated for 1 h. Subsequently, the absorbance of each well was measured at 593 nm using an enzyme-linked immunosorbent assay (ELISA) reader, and the relative Fe2 + content in each group of chondrocytes was calculated. Each experimental group was performed in triplicate.

Quantification of malondialdehyde (MDA) content in chondrocytes

Chondrocytes from each group were collected and washed three times with PBS following the protocol provided by the MDA kit (Elabscience, No. E-BC-K028-M). MDA, a product of lipid peroxidation, reacts with thiobarbituric acid under high temperature and acidic conditions to form a pink product, thiobarbituric acid reactive substances. Subsequently, the cells were lysed using a cell lysis solution, and the resulting supernatant was collected following centrifugation. A total of 0.2 mL of the supernatant was combined with 0.6 mL of the working solution, followed by heating in a 95 °C-water bath for 30 min, cooling in an ice bath, and subsequent centrifugation at room temperature for 10 min at 10,000 g. The resulting supernatant was collected, and the absorbance at 532 nm and 600 nm of each well was measured using an ELISA reader. The MDA content of each group was then calculated. The formula for calculating MDA content in cells is: MDA (nmol/mg protein) = (ΔA1/ΔA2) × C ÷ Cpr, where ΔA1 is the optical density (OD) of the test tube minus the OD of the blank tube, ΔA2 is the OD of the standard tube minus the OD of the blank tube, C is the concentration of the standard (10 nmol/mL), and Cpr is the protein concentration of the sample (mg protein/mL). Each experimental group was performed in triplicate.

Detection of intracellular ROS levels in chondrocytes using fluorescent probes

Chondrocytes from various groups were gently washed three times with PBS and then incubated with 10 μM of either DCFH-DA fluorescent probes in the dark at room temperature for 30 min. Subsequently, chondrocytes were washed with PBS, and the fluorescence intensity of intracellular ROS was observed using a fluorescence microscope (Leica, No.DM2500). Each experimental group was performed in triplicate.

Quantitative polymerase chain reaction (qPCR) detection

RNA was isolated using the TRIzol reagent provided by Aidlab (Catalog No. 252250AX), following a protocol optimized for chondrocyte samples. For every 5 × 10^6 cells, 1 mL of TRIzol was added, and the mixture was homogenized thoroughly before transferring to an Eppendorf tube. Chloroform was added in a ratio of 200 μL per 1 mL of TRIzol, followed by vigorous shaking for 15 s and standing for 3 min. The mixture was then centrifuged at 12,000 g for 15 min. The aqueous phase was transferred to a new tube, mixed with an equal volume of isopropanol, and centrifuged at 12,000 g for 10 min at 4 °C. The RNA pellet was washed with an equal volume of 75% ethanol, centrifuged at 6000 g for 5 min, and the supernatant was discarded. The RNA pellet was air-dried and dissolved in 20 μL of DEPC-treated water for further analysis. β-actin was selected as our reference gene for normalization. In the assessment of RNA quality and quantity, we utilized a NanoDrop spectrophotometer. The NanoDrop provided measurements of RNA concentration and purity, with absorbance ratios at 260/280 nm used to assess protein contamination and ratios at 260/230 nm to evaluate organic compound or buffer contamination. Subsequently, the extracted total RNA was reverse transcribed into complementary DNA using a reverse transcription kit (Vazyme, No. R101-01/02). The DNA amplification step was carried out using the Applied Biosystems 7500 Real-Time PCR system, and the obtained results were analyzed using the 2-ΔΔCq

Table 1 The primer sequences

Name	Primer	Sequence
β-actin	Forward	5′- TGTCCACCTTCCAGCAGATGT-3′
	Reverse	5′- AGCTCAGTAACAGTCCGCCTAGA-3′
Keap1	Forward	5′- TGGACTTTCGTAGCCTCCAT-3′
	Reverse	5′- GCATTCCACACTGTCCAGAA-3′
Nrf2	Forward	5′- CAGCATAGAGCAGGACATGGAG-3′
	Reverse	5′- GAACAGCGGTAGTATCAGCCAG-3′
GPX4	Forward	5′- CCTCTGCTGCAAGAGCCTCCC-3′
	Reverse	5′- CTTATCCAGGCAGACCATGTGC-3′
SLC7A11	Forward	5′- CTTTGTTGCCCTCTCCTGCTTC-3′
	Reverse	5′- CAGAGGAGTGTGCTTGTGGACA-3′
MMP13	Forward	5′- GCATTGGCTGAGTGAAAGAGAC-3′
	Reverse	5′- ATGATGAACGATGGACAGATGA-3′
ADAMTS-5	Forward	5′- ATGATTCGCCTCGGGGCTC-3′
	Reverse	5′- GCACTCTCCGAAGGGGATCT-3′
Col2a1	Forward	5′- GTGGAGGTGGACGCTACACTCA-3′
	Reverse	5′- AGCCAGGTTGCCATCGCCATA-3′
aggrecan	Forward	5′- ACCAGACTGTCAGATACCCC-3′
	Reverse	5′- CATAAAAGACCTCACCCTCC-3′

method. The primer sequences are listed in Table 1. Each experimental group was performed in triplicate.

Western blot (WB) analysis

Chondrocyte cells were washed gently with PBS, and then lysed using Radioimmunoprecipitation assay buffer containing 1% phenylmethylsulfonyl fluoride and 1% phosphatase inhibitor on ice. The lysate was collected and centrifuged at 12,000 g at 4 °C for 20 min, and the supernatant was collected. Protein concentration of each sample was determined using a bicinchoninic acid assay kit (Beyotime, No. P0012). For the standard curve, a series of bovine serum albumin standards ranging from 0 to 2000 μg/mL were prepared. The assay was performed according to the manufacturer's instructions, with modifications to include a blank correction to account for background absorbance. Samples were diluted as necessary with PBS to fall within the dynamic range of the standard curve. Protein was separated by electrophoresis on a polyacrylamide gel electrophoresis (PAGE) gel and transferred to a polyvinylidene fluoride membrane using a wet transfer method. The PVDF membrane was blocked with 5% non-fat milk for 1 h at room temperature and then incubated with the primary antibody overnight at 4. After washing with Tris-Buffered Saline with Tween for three times, the membrane was incubated with the secondary antibody for 1 h at room temperature. The protein bands were visualized and imaged using an imaging system (ChemiDoc™ XRS + System, Bio-Rad), and the intensity of each protein band was quantified (BandScan). The antibodies for WB are listed in Table 2.

In vivo experiments

Grouping and modeling of mice

All mice were housed in a clean-level animal facility. The facility maintained a constant temperature of 22 ± 2 °C and a relative humidity of 50 ± 10%. The light/dark cycle was set to 12 h light/12 h dark. The bedding material used was autoclaved aspen wood shavings. Additionally, the mice had ad libitum access to food and water. Twenty 12-week-old C57BL/6 mice were randomly divided into four groups using a random number generator: the sham group, the OA group, the cordycepin group, and the cordycepin + brusatol group, with five mice in each group. All groups, except the sham, were used to create an OA model. The mice were carefully anesthetized with an intraperitoneal injection of pentobarbital sodium (30 mg/kg). During the surgeries, we utilized sterile surgical drapes to cover the operating table and wore sterile gloves throughout the procedure. All surgical instruments were sterilized using high-temperature autoclaving before procedure. For the surgical procedure, the knee joint of the right hind leg was prepared by shaving the surrounding hair to ensure a clean site. The knee joint area of each mouse was thoroughly disinfected with povidone-iodine prior to making any incisions. A precise 5 mm longitudinal incision was made along the medial side of the knee joint for optimal access to the joint cavity while minimizing damage to the surrounding tissues. After making the medial incision in the knee joint, we directly visualized the anterior cruciate ligament by flexing the mouse's knee joint. This approach allowed us clear access to the ligament. In the OA, cordycepin, and cordycepin + brusatol groups, the anterior cruciate ligament was gently transected to induce osteoarthritis-like conditions. The incision was then meticulously sutured for proper healing. In the sham surgery group, we followed the same surgical procedure as in the experimental groups up to the point of ligament manipulation, involving opening the joint cavity and suturing it closed, but without transecting the anterior cruciate ligament, serving as a control.

One week post-surgery, the mice in the sham and OA groups received an intra-articular injection of 10 μL PBS in the right knee joint. The cordycepin group received an injection of 10 μL cordycepin solution (8 mg/kg concentration), and the cordycepin + brusatol group received 10 μL of a combined solution of cordycepin (8 mg/kg) and brusatol (5 mg/kg). Injections were administered weekly for a total of four weeks. Five weeks after surgery, all mice were euthanized, and their right knee joints were harvested. The tissues were then embedded in paraffin,

Table 2 The antibodies for western blotting

Classification	Name	Manufacturer	Catalog number	Dilution ratio
Primary antibodies	β-actin	Abcam	ab227387	1:1000
	Keap1	Abcam	ab119403	1:1000
	Nrf2	Affinity	AF7006	1:1000
	GPX4	Sigma-Aldrich	SAB5700944	1:1000
	SLC7A11	KALANG	kl410Ra21	1:1000
	MMP13	Abcam	ab219620	1:1000
	ADAMTS-5	Abcam	ab41037	1:1000
	Col2a1	Affinity	AF5456	1:1000
	aggrecan	Abcam	ab313636	1:1000
Secondary antibodies	HRP Conjugated AffiniPure Goat Anti-rabbit IgG (H + L)	Boster	BA1054	1:50000

sectioned, and stained with Safranin O, hematoxylin and eosin (HE), and subjected to immunohistochemistry and immunofluorescence experiments.

Evaluation of osteoarthritis degree using the osteoarthritis research society international (OARSI) score

The degree of osteoarthritis was evaluated using the OARSI score, which is determined by multiplying the OARSI grade by the OARSI stage. The OARSI grade is determined based on the following criteria:

Grade 0 indicates an intact joint surface.

Grade 1 represents mild fibrillation or swelling of the joint surface.

Grade 2 indicates moderate fibrillation with superficial cartilage loss, typically affecting approximately one-third of the stained cartilage surface.

Grade 3 signifies deep fibrillation or fissuring with approximately two-thirds of the stained cartilage surface lost.

Grade 4 denotes erosion with exposed subchondral bone.

Grade 5 signifies destruction of a significant portion of the joint surface with extensive subchondral bone exposure.

Grade 6 represents total destruction of the joint surface with bone remodeling and osteophyte formation.

The OARSI stage is determined based on the extent of joint involvement and is categorized as follows:

Stage 0 indicates no involvement.

Stage 1 represents involvement of less than 10% of the joint surface.

Stage 2 signifies involvement of 10–24% of the joint surface.

Stage 3 represents involvement of 25–49% of the joint surface.

Stage 4 denotes involvement of more than 50% of the joint surface.

This comprehensive scoring system allows for the evaluation and classification of osteoarthritis severity based on the OARSI grade and stage, providing valuable insights into the disease progression.

Statistical analysis

Quantitative data were presented as mean ± standard deviation, providing a comprehensive summary of the central tendency and variability. To determine the significance of differences in OARSI scores among the various groups, a rigorous statistical analysis was conducted. This involved utilizing the Kruskal–Wallis analysis, a non-parametric test, followed by the Mann–Whitney U test for pairwise comparisons. Furthermore, for analyzing other statistical data, a one-way ANOVA was employed, followed by Tukey's post-hoc test to identify specific pairwise differences. Notably, a significance level of $P < 0.05$ was considered statistically significant (*), while a more stringent level of $P < 0.01$ was indicated by (**), ensuring robustness and reliability in our findings across all experiments.

Results

Establishment and verification of the ferroptosis model

Initially, a ferroptosis model was established in chondrocytes by stimulating them with interleukin-1 beta (IL-1β) at a concentration of 10 ng/mL, and the model was subsequently validated. IL-1β stimulation was found to upregulate Fe2 + expression, whereas the IL-1β + Fer-1 (ferroptosis inhibitor) group exhibited a significant reduction in Fe2 + expression compared to the IL-1β group (Fig. 1a). Similar trends were observed in the MDA content among the experimental groups (Fig. 1b). Furthermore, ROS levels in chondrocytes were assessed (Fig. 1c, d). Following IL-1β stimulation,

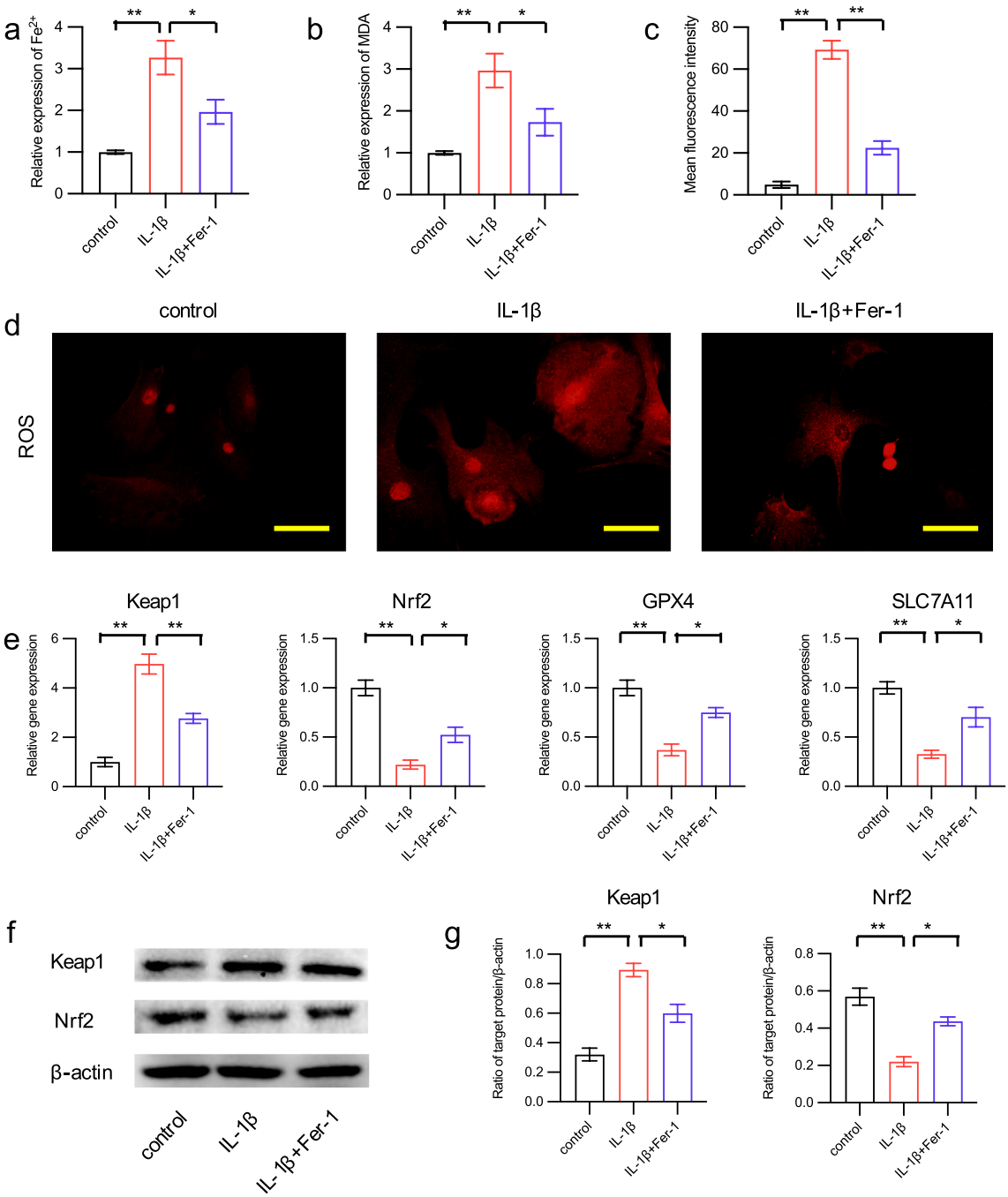

Fig. 1 Establishment and verification of ferroptosis model. **a**,**b** Detection of Fe2 + and MDA contents in chondrocytes. **c**,**d** Fluorescence images and intensity analysis of ROS in chondrocytes. bar = 20 μm. **e** qPCR analysis of Keap1, Nrf2, GPX4, and SLC7A11. **f** WB analysis of Keap1 and Nrf2. **g** Quantification of specific signal intensities. *$p < 0.05$, **$p < 0.01$, n = 3

an elevation in ROS levels was observed in chondrocytes, while treatment with Fer-1 demonstrated the ability to mitigate the effects induced by IL-1β. Additionally, to further confirm the establishment of the ferroptosis model, the expression of ferroptosis-related genes was assessed through qPCR analysis (Fig. 1e). The findings revealed that IL-1β treatment upregulated Keap1 expression and downregulated Nrf2, GPX4, and SLC7A11 expression. Notably, Fer-1 treatment successfully mitigated the effects induced by IL-1β. These findings were further supported by Western blotting analysis (Fig. 1g, h). Collectively, our results strongly

suggest that IL-1β stimulation at a concentration of 10 ng/mL can induce ferroptosis in chondrocytes.

Cordycepin inhibits chondrocyte ferroptosis

Cordycepin's toxicity on chondrocytes was assessed using a CCK-8 assay (Fig. 2a, b). Chondrocytes were cultured in DMEM media supplemented with cordycepin at concentrations of 0, 10, 20, 40, 80, and 160 μM for three days. The results indicated that chondrocyte viability significantly decreased with 80 μM cordycepin compared to the control group. Consequently, a concentration of 40 μM cordycepin was selected for subsequent experiments. Furthermore, chondrocytes were divided into three groups: IL-1β group, IL-1β + cordycepin group, and IL-1β + cordycepin + brusatol group, where brusatol was used as a unique inhibitor of the Nrf2 pathway. Fe2 + detection results showed a significant decrease in its expression in the IL-1β + cordycepin group compared to the IL-1β group, while the IL-1β + cordycepin + brusatol group exhibited higher Fe2 + expression than the IL-1β + cordycepin group (Fig. 2c). Similar trends were observed in MDA detection (Fig. 2d). Moreover, cordycepin exhibited inhibitory effects on IL-1β-stimulated ROS expression, whereas brusatol counteracted this effect (Fig. 2e, f). Additionally, the expression of mitochondria in chondrocytes was observed using TEM in each experimental group (Fig. 2g). Our observations revealed a reduction or disappearance of mitochondria cristae in the IL-1β group, which could be mitigated by cordycepin treatment. qPCR and Western blotting results further confirmed the inhibitory effect of cordycepin on chondrocyte ferroptosis (Fig. 2h-j). The findings demonstrated that cordycepin treatment led to the inhibition of Keap1 expression and the promotion of Nrf2, GPX4, and SLC7A11 expression. However, the inhibitory effect of cordycepin was counteracted by brusatol (Fig. 2h-j).

Cordycepin attenuates chondrocyte matrix degradation

The effect of cordycepin on the matrix of chondrocytes was investigated by examining the expression of matrix metalloproteinase 13 (MMP13), a disintegrin and metalloproteinase with thrombospondin motifs 5 (ADAMTS-5), collagen type II alpha 1 chain(col2a1), and aggrecan genes using qPCR in the IL-1β group, IL-1β + cordycepin group, and IL-1β + cordycepin + brusatol group (Fig. 3a). Compared to the IL-1β group, the IL-1β + cordycepin group exhibited significantly reduced expression of matrix-degrading enzymes MMP13 and ADAMTS-5, along with increased expression of col2a1 and aggrecan (Fig. 3a). WB analysis demonstrated similar findings (Fig. 3b, c). These findings suggest that cordycepin inhibits matrix degradation in chondrocytes. Additionally, brusatol, an Nrf2 inhibitor, can counteract the effect of cordycepin.

Cordycepin inhibits ferroptosis of chondrocytes in vivo

A mouse model of osteoarthritis was established, and the mice were divided into the sham group, OA group, cordycepin group, and cordycepin + brusatol group. Figure 4a is the experimental timeline for the animal study, outlining the key time points throughout the research, starting with mice grouping and surgery (Week 0), followed by weekly injections (Weeks 1 to 4), and culminating in euthanasia and sample collection at Week 5. Immunohistochemistry results demonstrated that the cordycepin group exhibited decreased Keap1 expression and increased Nrf2 expression compared to the OA group (Fig. 4b–e). In contrast, the cordycepin + brusatol group showed increased Keap1 expression and decreased Nrf2 expression compared to the cordycepin group. The results were further confirmed using immunofluorescence (Fig. 4f–i). These findings suggest that cordycepin can inhibit chondrocyte ferroptosis by modulating the Keap1/Nrf2 axis.

Cordycepin inhibits osteoarthritis in vivo

Immunohistochemistry was conducted to assess the expression of col2a1 and aggrecan in the sham, OA, cordycepin, and cordycepin + brusatol groups (Fig. 5a–d). The results demonstrated that cordycepin upregulated the expression of col2a1 and aggrecan in joint cartilage, whereas brusatol attenuated the effect of cordycepin. Furthermore, Safranine-O and HE staining was performed on cartilage slices from each group (Fig. 5e). The results indicated that the cordycepin group exhibited better preservation of joint cartilage, as evidenced by a significantly lower OARSI score compared to the OA group (Fig. 5f). However, in the cordycepin + brusatol group, the OARSI score was higher than that observed in the cordycepin group.

Discussion

The present study aimed to investigate the potential therapeutic effects of cordycepin on OA by inhibiting chondrocyte ferroptosis via the Keap1/Nrf2 signaling pathway. Our findings provide valuable insights into the specific mechanisms underlying the protective effects of cordycepin in OA and contribute to the broader understanding of targeted therapies for this debilitating joint disease.

Ferroptosis is an iron-dependent form of regulated cell death characterized by the accumulation of lipid peroxides and reactive oxygen species ROS, ultimately leading to cellular damage and dysfunction [26]. Emerging

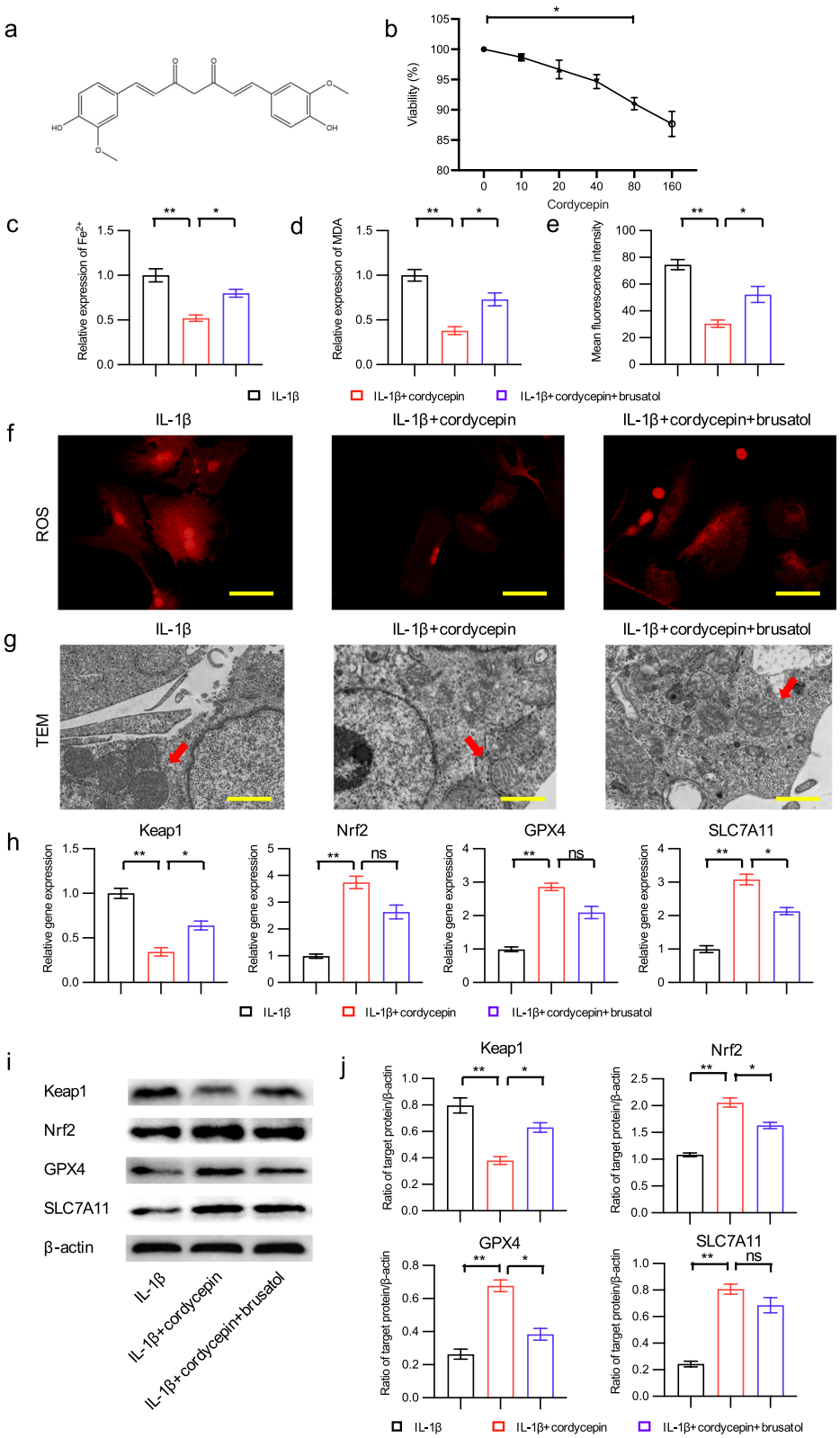

Fig. 2 Cordycepin inhibits chondrocyte ferroptosis. **a** Molecular formula of cordycepin. **b** CCK-8 assay for cordycepin cytotoxicity in chondrocytes. **c**,**d** Detection of Fe2 + and MDA contents in chondrocytes. **e**,**f** Fluorescence images and intensity analysis of ROS in chondrocytes. bar = 20 μm. **g** TEM images of chondrocytes in different groups. **h** qPCR analysis of Keap1, Nrf2, GPX4, and SLC7A11. **i** WB analysis of Keap1, Nrf2, GPX4, and SLC7A11. **j** Quantification of specific signal intensities. *$p < 0.05$, **$p < 0.01$, n = 3

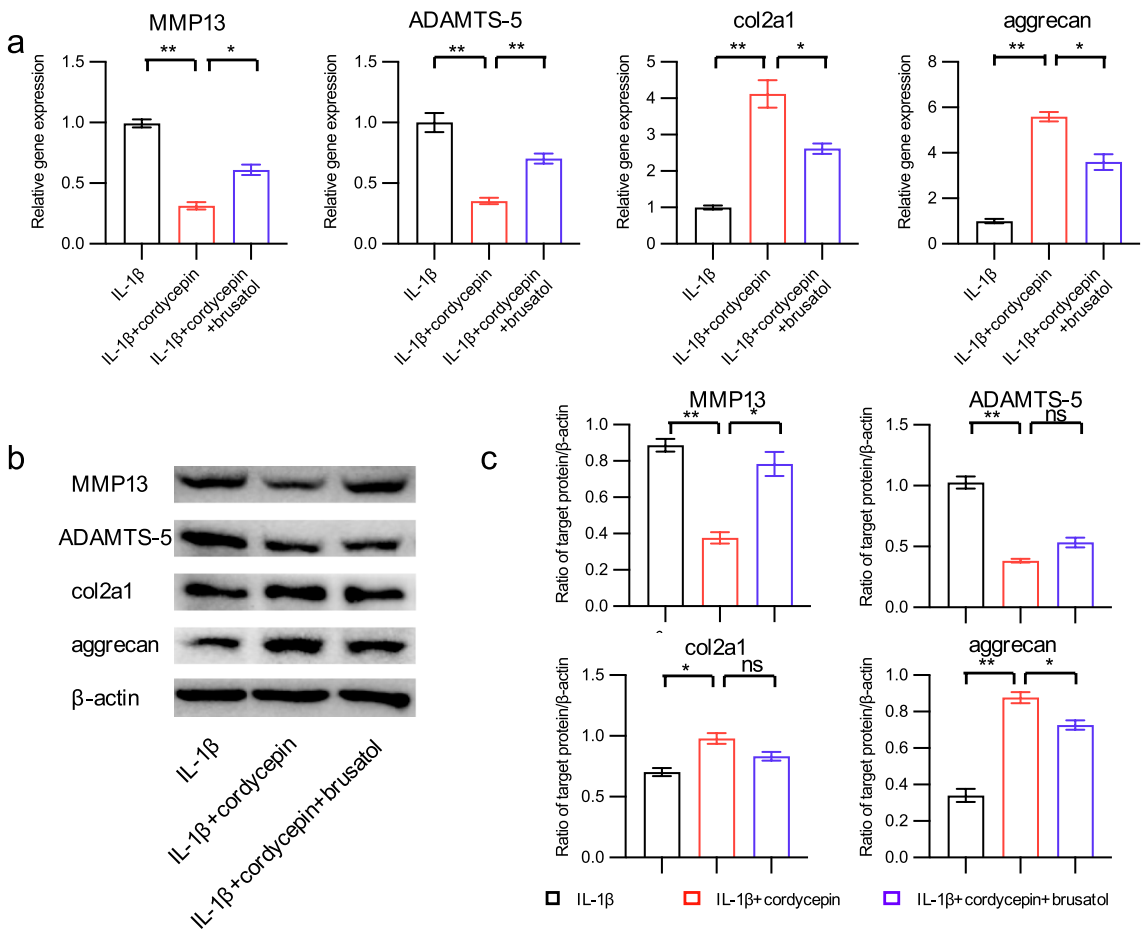

Fig. 3 Cordycepin inhibits chondrocyte matrix degradation. **a** PCR analysis of MMP13, ADAMTS-5, Col2a1, and Aggrecan. **b** WB analysis of MMP13, ADAMTS-5, Col2a1, and Aggrecan. **c** Quantification of specific signal intensities. *$p < 0.05$, **$p < 0.01$, n = 3

evidence suggests that ferroptosis plays a critical role in the pathogenesis of OA, contributing to the progressive degradation of articular cartilage [27, 28]. Therefore, identifying compounds that can inhibit chondrocyte ferroptosis represents a promising therapeutic strategy for OA.

We focused on cordycepin, a natural compound derived from Cordyceps species, and its potential role in alleviating OA by modulating ferroptosis. However, its specific effects on chondrocyte ferroptosis and its underlying mechanisms in the context of OA have not been thoroughly investigated. Our results demonstrated that cordycepin treatment significantly reduced the expression of iron metabolism-related proteins and oxidative stress markers in chondrocytes, indicating its inhibitory effect on ferroptosis. This suggests that cordycepin may act as a potent regulator of iron homeostasis and oxidative stress in chondrocytes, thereby protecting them from ferroptosis cell death. Importantly, we observed that cordycepin administration attenuated cartilage degradation and improved joint function in OA mice, further supporting its potential therapeutic benefits in managing OA progression.

(See figure on next page.)

Fig. 4 Cordycepin inhibits ferroptosis of chondrocytes in vivo. **a** The experimental timeline for the animal study. **b** Immunohistochemical staining for Keap1 in mouse joint cartilage sections. bar = 200 μm. **c** Quantification of Keap1-positive cells. **d** Immunohistochemical staining for Nrf2 in mouse joint cartilage sections. bar = 200 μm. **e** Quantification of Nrf2-positive cells. **f** Immunofluorescence staining for Keap1 in joint cartilage. bar = 100 μm. **g** Quantification of Keap1-positive cells. **h** Immunohistochemical staining for Nrf2 in joint cartilage. bar = 100 μm. **i** Quantification of Nrf2-positive cells. *$p < 0.05$, **$p < 0.01$, n = 3

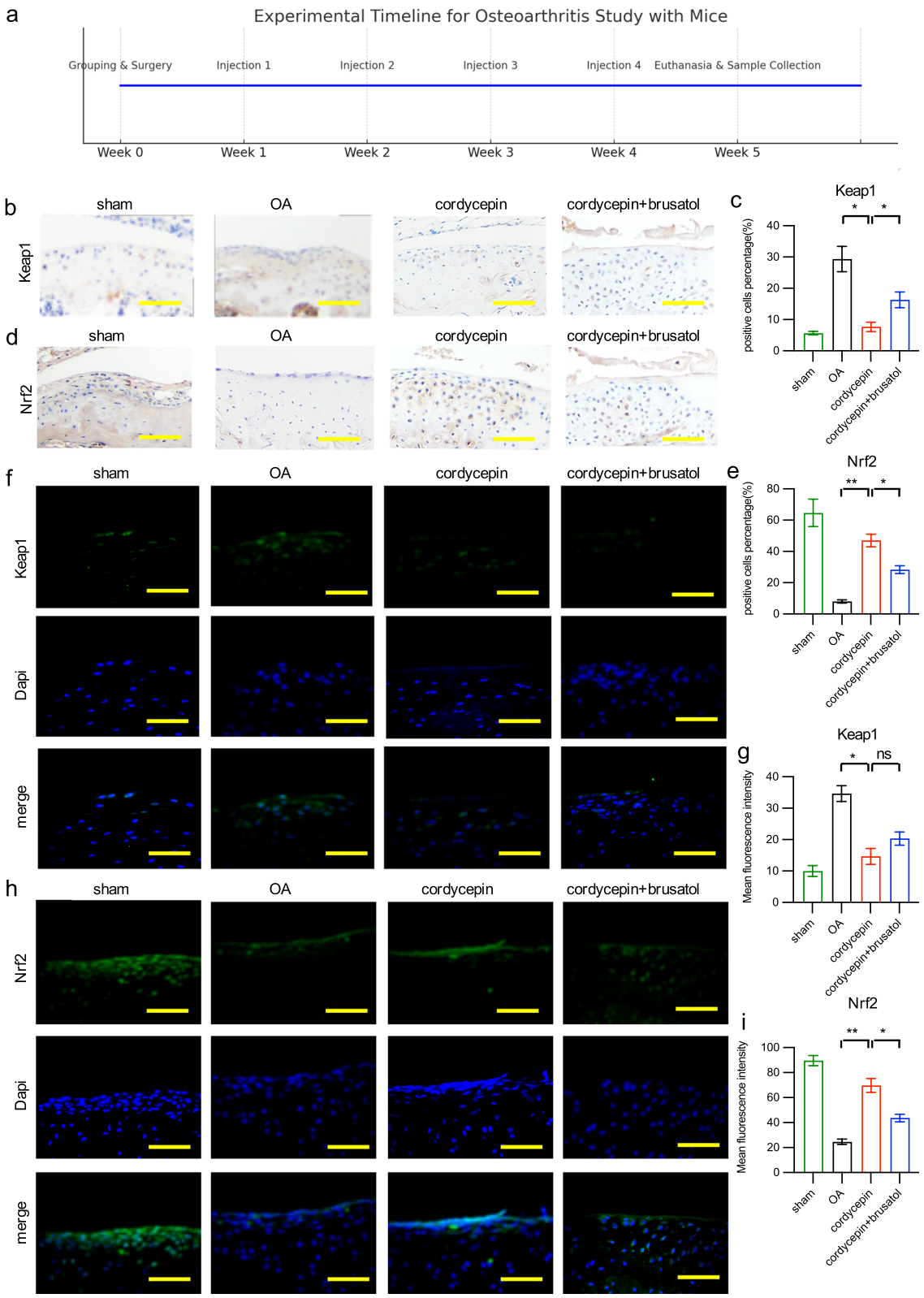

Fig. 4 (See legend on previous page.)

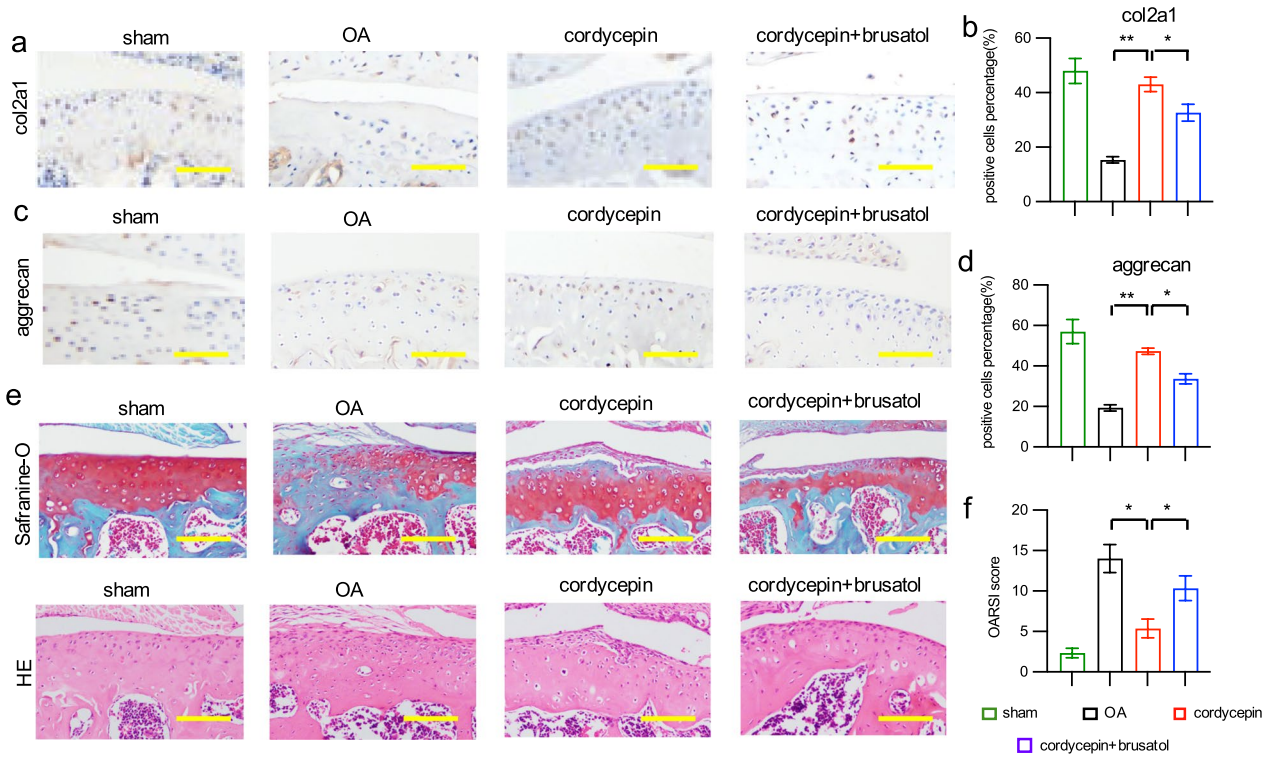

Fig. 5 Cordycepin inhibits osteoarthritis in vivo. **a** Immunohistochemical staining for Col2a1 in joint cartilage. bar = 200 μm. **b** Quantification of Col2a1-positive cells. **c** Immunohistochemical staining for Aggrecan in joint cartilage. bar = 200 μm. **d** Quantification of Aggrecan-positive cells. **e** Safranine-O and HE staining of joint cartilage. bar = 200 μm. **f** OARSI scores of joint cartilages. *$p < 0.05$, **$p < 0.01$, n = 3

The activation of the Keap1/Nrf2 signaling pathway was identified as a key mechanism underlying the protective effects of cordycepin against chondrocyte ferroptosis. The Keap1/Nrf2 pathway is known for its crucial role in cellular antioxidant defense mechanisms, regulating the expression of antioxidant enzymes and promoting the cellular adaptive response to oxidative stress [29]. Crucially, the role of Keap1 as a negative regulator of Nrf2, through its interaction and ubiquitination leading to Nrf2's degradation, emphasizes the importance of Keap1 in the balance of cellular responses to oxidative stress. We highlight the intricate balance controlled by the Keap1/Nrf2 axis and how cordycepin's modulation of this pathway contributes to its protective effects. Specifically, our findings suggest that cordycepin interferes with the Keap1-mediated degradation of Nrf2, thereby enhancing the cellular defense against oxidative stress and ferroptosis.

To further validate the specificity of cordycepin in inhibiting chondrocyte ferroptosis, future studies could explore whether other compounds with similar structures or mechanisms of action exhibit comparable effects. Comparing the efficacy of cordycepin with other potential ferroptosis inhibitors would provide valuable insights into its specificity and potential advantages in the context of OA treatment.

Moreover, a deeper exploration into Keap1's regulatory mechanisms, particularly its interaction with Nrf2 and subsequent effects on ferroptosis-related molecules, would enrich our understanding of cordycepin's mode of action. Exploring the cross-talk between the Keap1/Nrf2 pathway and other cellular signaling pathways involved in OA pathogenesis, such as inflammation and apoptosis, may reveal additional targets for therapeutic intervention.

It is important to acknowledge the limitations of the current investigation. Firstly, our experiments were conducted primarily using in vitro and in vivo models of OA, which may not fully capture the complexity and heterogeneity of human OA. Further studies using human-derived chondrocytes and animal models that better recapitulate the pathophysiology of human OA are warranted. Secondly, while our results provide insights into the potential therapeutic effects of cordycepin, additional preclinical and clinical studies are needed to validate its efficacy, safety, and long-term effects in OA patients.

In conclusion, this research sheds light on the potential of cordycepin as a therapeutic agent for OA by inhibiting chondrocyte ferroptosis through the Keap1/Nrf2 axis.

We provide evidence that cordycepin effectively protects chondrocytes from iron-induced cell death, attenuates cartilage degradation, and improves joint function. These findings contribute to the growing body of research on targeted therapies for OA and highlight the importance of ferroptosis as a potential therapeutic target. Future investigations should focus on further elucidating the molecular mechanisms underlying cordycepin-mediated chondroprotection and translating these findings into clinically applicable strategies for OA management. Ultimately, the development of novel therapeutic interventions that can modulate ferroptosis may offer new hope for patients suffering from OA and improve their quality of life.

Conclusion

This research demonstrates the significant therapeutic potential of the ROS-responsive hydrogel loaded with garlic extract in mitigating IVDD. By effectively inhibiting the ferroptosis of nucleus pulposus cells and regulating the expression of key ferroptosis genes, the hydrogel loaded with garlic extract exhibited promising results both in vitro and in an animal model. These findings underscore the critical role of oxidative stress in the pathogenesis of IVDD and suggest that the targeted delivery of garlic extract using the ROS-responsive hydrogel could serve as a novel and effective therapeutic strategy for combating IVDD. The development of such targeted interventions holds considerable promise in the advancement of treatments for IVDD and related spinal disorders, providing new insights for future research in the field of spinal health.

Abbreviations

IVDD	Intervertebral disc degeneration
ROS	Reactive oxygen species
OA	Osteoarthritis
Keap1	Kelch-like ECH-associated protein 1
Nrf2	Nuclear factor erythroid 2-related factor 2
ARE	Antioxidant response element
HO-1	Heme oxygenase-1
GPx	Glutathione peroxidase
SLC7A11	Solute carrier family 7 member 11
PBS	Phosphate-Buffered Saline
DMEM	Dulbecco's Modified Eagle's Medium
FBS	Fetal Bovine Serum
MDA	Malondialdehyde
ELISA	Enzyme-linked immunosorbent assay
qPCR	Quantitative polymerase chain reaction
WB	Western blot
PAGE	Polyacrylamide gel electrophoresis
OARSI	Osteoarthritis research society international
IL-1β	Interleukin-1 beta
MMP13	Matrix metalloproteinase 13
ADAMTS-5	A disintegrin and metalloproteinase with thrombospondin motifs 5
col2a1	Collagen type II alpha 1 chain
CCK-8	Cell Counting Kit-8

Acknowledgements
Not applicable.

Author contributions
JL contributed to study conception and drafted the manuscript. JL and ZL conducted the literature review, performed analysis, and acquired the data.

Funding
This study was supported by the Foundation of the Natural Science Foundation of Zhejiang Province (No.Q19H60007).

Availability of data and materials
The datasets generated and analyzed during the current study are available from the corresponding author on reasonable request.

Declarations

Ethics approval and consent to participate
This study was approved by permission from the Ethics Committee of Shaoxing People's Hospital (Approval No. 2021-034).

Consent for publication
Not applicable.

Competing interests
The authors declare that no conflict of interest exists.

Received: 17 October 2023 Accepted: 21 February 2024
Published online: 28 February 2024

References

1. Sacitharan PK (2019) Ageing and osteoarthritis. Subcell Biochem 91:123–159. https://doi.org/10.1007/978-981-13-3681-2_6
2. Mandl LA (2019) Osteoarthritis year in review 2018: clinical. Osteoarthritis Cartilage 27(3):359–364. https://doi.org/10.1016/j.joca.2018.11.001
3. Abramoff B, Caldera FE (2020) Osteoarthritis: pathology, diagnosis, and treatment options. Med Clin North Am 104(2):293–311. https://doi.org/10.1016/j.mcna.2019.10.007
4. Li J, Cao F, Yin HL et al (2020) Ferroptosis: past, present and future. Cell Death Dis 11(2):88. https://doi.org/10.1038/s41419-020-2298-2
5. Jakaria M, Belaidi AA, Bush AI, Ayton S (2021) Ferroptosis as a mechanism of neurodegeneration in Alzheimer's disease. J Neurochem 159(5):804–825. https://doi.org/10.1111/jnc.15519
6. Koppula P, Zhuang L, Gan B (2021) Cystine transporter SLC7A11/xCT in cancer: ferroptosis, nutrient dependency, and cancer therapy. Protein Cell 12(8):599–620. https://doi.org/10.1007/s13238-020-00789-5
7. Fang X, Ardehali H, Min J, Wang F (2023) The molecular and metabolic landscape of iron and ferroptosis in cardiovascular disease. Nat Rev Cardiol 20(1):7–23. https://doi.org/10.1038/s41569-022-00735-4
8. Ulasov AV, Rosenkranz AA, Georgiev GP, Sobolev AS (2022) Nrf2/Keap1/ARE signaling: towards specific regulation. Life Sci 291:120111. https://doi.org/10.1016/j.lfs.2021.120111
9. Bellezza I, Giambanco I, Minelli A (1865) Donato R (2018) Nrf2-Keap1 signaling in oxidative and reductive stress. Biochim Biophys Acta Mol Cell Res 5:721–733. https://doi.org/10.1016/j.bbamcr.2018.02.010
10. Yu C, Xiao JH (2021) The keap1-Nrf2 system: a mediator between oxidative stress and aging. Oxid Med Cell Longev 2021:6635460. https://doi.org/10.1155/2021/6635460
11. Lu MC, Ji JA, Jiang ZY, You QD (2016) The Keap1-Nrf2-ARE pathway as a potential preventive and therapeutic target: an update. Med Res Rev 36(5):924–963. https://doi.org/10.1002/med.21396
12. Li J, Lu K, Sun F et al (2021) Panaxydol attenuates ferroptosis against LPS-induced acute lung injury in mice by Keap1-Nrf2/HO-1 pathway. J Transl Med 19(1):96. https://doi.org/10.1186/s12967-021-02745-1

13. Sun X, Ou Z, Chen R et al (2016) Activation of the p62-Keap1-NRF2 pathway protects against ferroptosis in hepatocellular carcinoma cells. Hepatology 63(1):173–184. https://doi.org/10.1002/hep.28251
14. Xia M, Zhang Q, Zhang Y et al (2022) Growth differentiation factor 15 regulates oxidative stress-dependent ferroptosis post spinal cord injury by stabilizing the p62-Keap1-Nrf2 signaling pathway. Front Aging Neurosci 14:905115. https://doi.org/10.3389/fnagi.2022.905115
15. Fu F, Lai Q, Hu J et al (2022) Ruscogenin alleviates myocardial ischemia-induced ferroptosis through the activation of BCAT1/BCAT2. Antioxidants (Basel) 11(3):583. https://doi.org/10.3390/antiox11030583
16. Wan Y, Shen K, Yu H, Fan W (2023) Baicalein limits osteoarthritis development by inhibiting chondrocyte ferroptosis. Free Radic Biol Med 196:108–120. https://doi.org/10.1016/j.freeradbiomed.2023.01.006
17. Ashraf SA, Elkhalifa AEO, Siddiqui AJ et al (2020) Cordycepin for health and wellbeing: a potent bioactive metabolite of an entomopathogenic cordyceps medicinal fungus and its nutraceutical and therapeutic potential. Molecules. https://doi.org/10.3390/molecules25122735
18. Lan T, Yu Y, Zhang J et al (2021) Cordycepin ameliorates nonalcoholic steatohepatitis by activation of the AMP-activated protein kinase signaling pathway. Hepatology 74(2):686–703. https://doi.org/10.1002/hep.31749
19. Wei P, Wang K, Luo C et al (2021) Cordycepin confers long-term neuroprotection via inhibiting neutrophil infiltration and neuroinflammation after traumatic brain injury. J Neuroinflammation 18(1):137. https://doi.org/10.1186/s12974-021-02188-x
20. Yoon SY, Park SJ, Park YJ (2018) The anticancer properties of cordycepin and their underlying mechanisms. Int J Mol Sci 19(10):3027. https://doi.org/10.3390/ijms19103027
21. Radhi M, Ashraf S, Lawrence S et al (2021) A systematic review of the biological effects of cordycepin. Molecules 26(19):5886. https://doi.org/10.3390/molecules26195886
22. Xia C, Chen P, Mei S et al (2017) Photo-crosslinked HAMA hydrogel with cordycepin encapsulated chitosan microspheres for osteoarthritis treatment. Oncotarget 8(2):2835–2849. https://doi.org/10.18632/oncotarget.13748
23. Ying X, Peng L, Chen H, Shen Y, Yu K, Cheng S (2014) Cordycepin prevented IL-beta-induced expression of inflammatory mediators in human osteoarthritis chondrocytes. Int Orthop 38(7):1519–1526. https://doi.org/10.1007/s00264-013-2219-4
24. Hu P, Chen W, Bao J, Jiang L, Wu L (2014) Cordycepin modulates inflammatory and catabolic gene expression in interleukin-1beta-induced human chondrocytes from advanced-stage osteoarthritis: an in vitro study. Int J Clin Exp Pathol 7(10):6575–6584. https://doi.org/10.3389/fphar.2019.00715
25. Wang Z, Chen Z, Jiang Z et al (2019) Cordycepin prevents radiation ulcer by inhibiting cell senescence via NRF2 and AMPK in rodents. Nat Commun 10(1):2538. https://doi.org/10.1038/s41467-019-10386-8
26. Stockwell BR, Jiang X, Gu W (2020) Emerging mechanisms and disease relevance of ferroptosis. Trends Cell Biol 30(6):478–490. https://doi.org/10.1016/j.tcb.2020.02.009
27. Wang X, Liu Z, Peng P, Gong Z, Huang J, Peng H (2022) Astaxanthin attenuates osteoarthritis progression via inhibiting ferroptosis and regulating mitochondrial function in chondrocytes. Chem Biol Interact 366:110148. https://doi.org/10.1016/j.cbi.2022.110148
28. Zhang S, Xu J, Si H, Wu Y, Zhou S, Shen B (2022) The role played by ferroptosis in osteoarthritis: evidence based on iron dyshomeostasis and lipid peroxidation. Antioxidants (Basel) 11(9):1668. https://doi.org/10.3390/antiox11091668
29. Tu W, Wang H, Li S, Liu Q, Sha H (2019) The anti-inflammatory and anti-oxidant mechanisms of the keap1/Nrf2/ARE signaling pathway in chronic diseases. Aging Dis 10(3):637–651. https://doi.org/10.14336/AD.2018.0513

Publisher's Note